Unconventional line defects engineering in two-dimensional boron monolayers

Shao-Gang Xu,[1] Chang-Chun He,[2] Yu-Jun Zhao,[2] Hu Xu,[1,*] and Xiao-Bao Yang[2,†]

[1]*Department of Physics, Guangdong Provincial Key Laboratory of Computational Science and Material Design, Guangdong-Hong Kong-Macao Joint Laboratory for Photonic-Thermal-Electrical Energy Materials and Devices, Southern University of Science and Technology, Shenzhen 518055, People's Republic of China*

[2]*Department of Physics, South China University of Technology, Guangzhou 510640, People's Republic of China*

(Received 20 January 2021; accepted 16 April 2021; published 29 April 2021)

Line defects (LDs) are a kind of lattice imperfection widely existing in two-dimensional materials, which may play a significant role in the properties of materials. Different from the negative effect of LDs for stability in most 2D materials, we have proposed a simple universal rule to construct stable 2D boron isomers based on the LDs engineering, where the self-assembled monolayers are unconventionally enhanced. Based on the self-assembly of LDs from β_{12} and χ_3 monolayers, we have found several boron monolayers with higher stability on the Ag (111) substrate than the experimental phases, and two monolayers in our prediction have been confirmed by the recent experiments. Notably, the mechanical response of the boron monolayers also can be enhanced by the LDs, indicating the potential application for advanced flexible electronic devices.

DOI: 10.1103/PhysRevMaterials.5.044003

I. INTRODUCTION

Atomic defects have been widely investigated in three-dimensional (3D) bulk crystalline structures for decades, especially in the semiconductor industry; just one additional dopant atom per hundred million host atoms may dramatically alter the electronic properties of the host material. With the rapid development of nanoscience, various atomic defects also have been clearly characterized in two-dimensional (2D) materials, which are based on the application of the high-resolution transmission electron microscopy and the elaborate first-principles calculations [1,2]. As a typical extended topological defect, the line defect (LD) is a widespread inevitable structural imperfection induced by a symmetry-broken process in the large-scale growth of various 2D materials, which is pivotal in understanding the structure-property relationship and the device performance of 2D materials [3]. The theoretical calculations have proved that the inclusion of LDs in the 2D materials would induce higher formation energy [4–6], which indicates the energy unfavorable of the topological line defects.

Different from the traditional 2D crystals with well-defined lattices, the stable boron monolayers have been predicted to be a 2D pseudoalloy of triangles and hexagons [7–9], in which the potential stable boron monolayers are derived from the triangular lattice with hexagonal vacancies distributions [10,11]. In the experimental growth process, the actual patterns of boron monolayers are dependent on the activity of the metal substrates and the experimental conditions [12,13]. If we consider the easy synthesis of large-scale (high-quality) samples, moderate boron-metal interaction is a key factor. The Ag (111) substrate is found to be an ideal candidate, which has been verified by theories and experiments [14–17] for the single-crystal β_{12} (vacancy density $\upsilon = 1/6$), χ_3 ($\upsilon = 1/5$) and the metastable phase α monolayers [15,18]. Recently, Liu and colleagues demonstrated that the vacancy line defects in β_{12} and χ_3 could coexist on the Ag (111) substrates and self-assemble into new crystalline phases [19]. In addition, various energetically preferred LDs self-assembled in boron monolayers have been clearly observed by the functionalized probes [20,21]. Thus, due to the highly flexible bonding configurations (from two-center bonds to multicenter bonds) between boron atoms [22,23], the LDs in boron monolayers may induce a more fascinating structure-property relationship, which deserves a systematic research.

In this work, combined with the first-principles calculations, we have revealed a universal rule to construct various stable boron monolayers with LDs based on the self-assembly of α ribbons. Adopting a detailed electronic bonding analysis, we have uncovered the positive role of LDs to the stability of boron monolayers. In addition, the boron monolayers based on the self-assembly of LDs from β_{12} (A) and χ_3 (B) monolayers have been systematically explored, and several boron monolayers exhibit higher stability on Ag (111) substrates than the experimental phases. In particular, the designed boron monolayers with LDs reveal unusual higher mechanical response, which indicates a new platform for the applications in flexible electronic devices.

II. COMPUTATIONAL METHODS

All the first-principles calculations were performed based on density-functional theory as implemented in the Vienna *Ab initio* Simulation Package (VASP) [24]. The electron-ion

*xuh@sustech.edu.cn
†scxbyang@scut.edu.cn

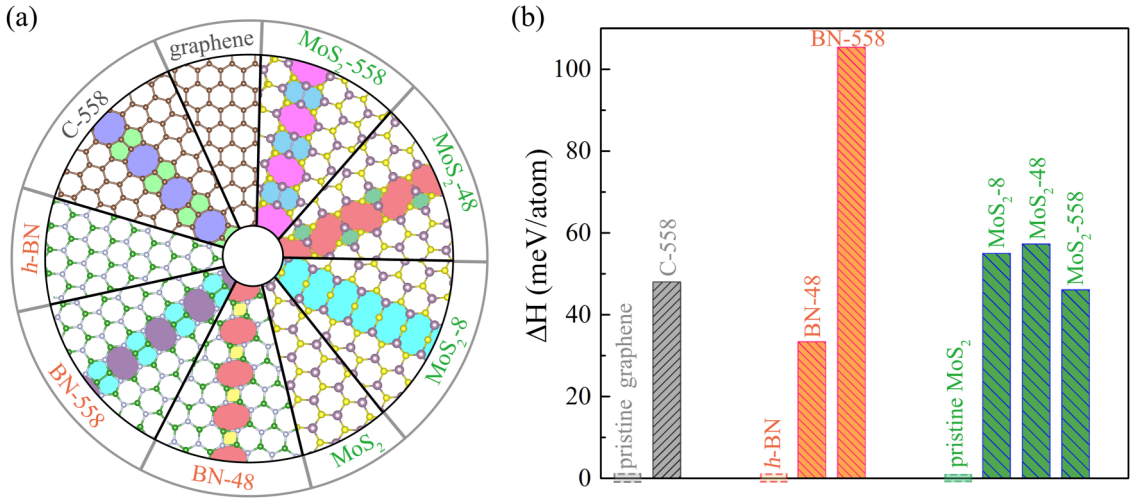

FIG. 1. (a) Top view of the typical LDs in graphene, *h*-BN, and MoS_2. (b) The relative formation energy of the LDs, where the corresponding pristine phases were set to zero point.

interactions were described by the projector augmented wave potentials [25]. To treat the exchange-correlation interaction of electrons, we chose the generalized gradient approximation of the Perdew-Burke-Ernzerhof functional [26]. The kinetic energy cutoff was set to 480 eV for the plane-wave expansion, and the forces acting on each atom were less than 0.01 eV $Å^{-1}$ to ensure the fully relaxed initial structures. A large vacuum region of 20 Å along the z direction was adopted for the 2D boron monolayers model to isolate neighboring periodic images. The thermal stability of the boron monolayer was carried out by the *ab initio* molecular dynamics (AIMD) simulations with a Nosé heat-bath scheme at given temperature [27]. In order to calculate the relative formation energy, the LDs in Fig. 1 were embedded in the ribbon model with a width larger than 30 Å [4,6].

The average formation energy (E_{form}) of the free-standing boron monolayers is defined as

$$E_{\text{form}} = (E_{\text{monolayer}}/n - E_{\text{at}}), \tag{1}$$

where $E_{\text{monolayer}}$ is the total energy of the boron monolayer, E_{at} is the energy of an isolated spin-polarized boron atom, and n is the number of B atoms in the cell.

In order to simulate the boron monolayers growth on the Ag (111) substrates, here we use a five-layer slab with the bottom two layers fixed to model the Ag (111) substrate and put the possible boron monolayers on the substrates with the absolute value of lattice mismatch under 2.5%. The average formation energy of the boron monolayers on the metal substrates is defined as

$$E_{\text{form}} = \frac{1}{n}(E_{\text{tot}} - E_{\text{sub}} - n \times \mu_{\text{B}}), \tag{2}$$

where the E_{tot}, E_{sub} represent the total energy of the B/Ag systems and the Ag (111) substrates respectively, n is the number of B atoms in the boron monolayers, and μ_{B} is the energy per atom in the boron solid of α phase. In addition, the definition of the orientation-dependent mechanical response is presented in the Supplemental Material (SM) [28].

III. RESULTS AND DISCUSSION

Compared to the 3D bulk materials, 2D crystals with reduced dimensionality usually show various fascinating properties and can act as an ideal platform for fundamental research and device design [29,30]. However, the desired crystalline order in 2D is highly susceptible to various types of fluctuation [31], which would hinder the production of large-scale 2D single-crystalline phases. As a typical 2D defect, different LDs have been reported in the epitaxial growth of 2D crystalline domains [3] due to the in-plane structural anisotropy or the varying lattice orientation of the substrates [1,3]. Herein, we have studied the LDs in 2D semimetal (graphene), insulator (*h*-BN), and semiconductor (MoS_2), including the extended 5-5-8 type LDs in graphene [32], the (4-8 type/5-5-8 type) LDs in *h*-BN and MoS_2 [see Fig. 1(a)] [6,33–35]. As shown in Fig. 1(b), compared with the pristine 2D single crystalline, the included extended LDs weaken the structural stability of the systems. For the 5-5-8 type LDs in graphene, the former calculated binding energy is 46.3 meV/atom higher than the pristine graphene based on a ribbon model of 29.7 Å [4], and our calculated relative average formation energy is 48 meV/atom [see Fig. 1(b)], which indicates the reliability of our results. The former research also proposed that the excellent mechanical performance of the pristine 2D materials would be decreased by the presence of the topological defects [36–38], indicating the negative role of LDs for stability of the conventional 2D materials.

The story in boron monolayers may be different from other 2D materials due to its unique characteristics: (i) the flexible bonding configurations (from two-center bonds to multicenter bonds) between boron atoms lead to the natural polymorphism [10,39]; (ii) the variety of properties are modulated by the structural diversity [40,41]; and (iii) the growth patterns of boron monolayers are dependent on the substrates and the experimental conditions [13,15,42,43]. For the first issue, all the theoretical explorations in the past decades lead to a similar conclusion: (i) the potential boron monolayer isomers are composed of triangular and hexagonal motifs; (ii) the

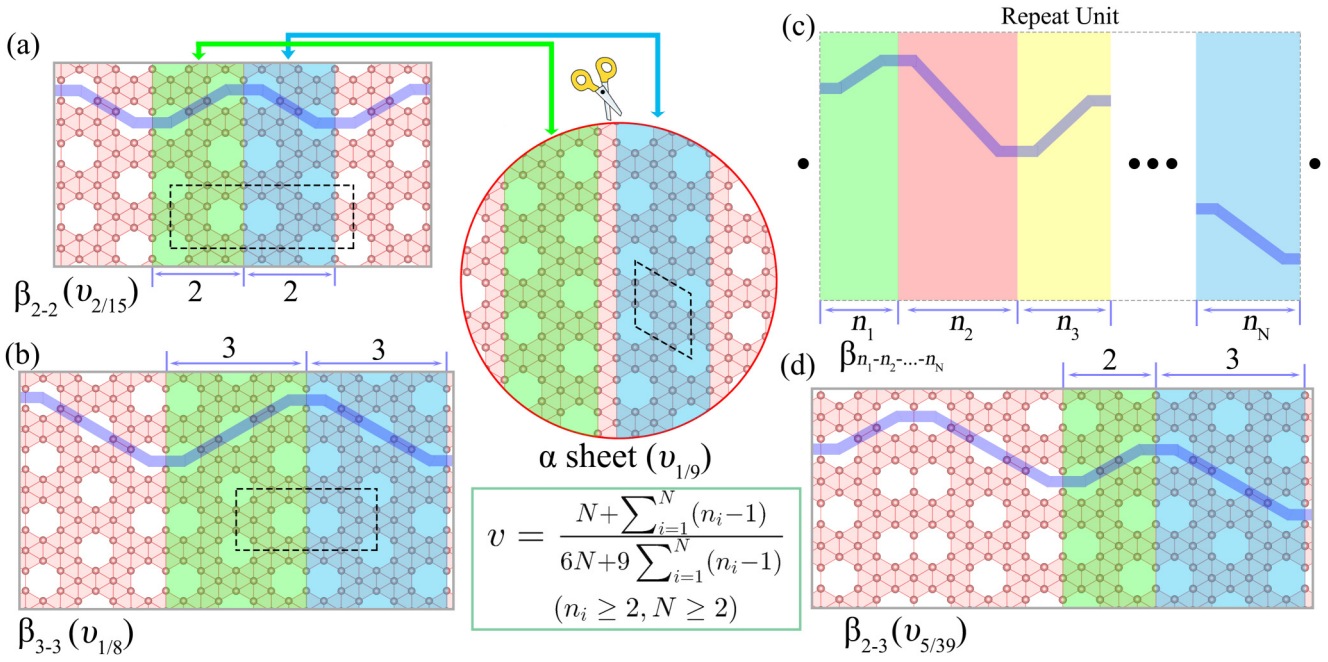

FIG. 2. (a) The sketch map of the formation of β_{2-2} monolayer based on the α ribbons self-assembly. (b) The similar formation mechanism of β_{3-3} monolayer. (c) The schematic diagram of constructing any $\beta_{n_1-n_2-\ldots-n_N}$ monolayer based on the α ribbons self-assembly. (d) represents a long-range order candidate of β_{2-3} monolayer. The black dashed lines in (a), (b) mark the unit cell of the monolayer.

energetic boron monolayers lie in a narrow range of $1/9 \leqslant \upsilon \leqslant 1/7$ [39]. Various theoretical investigations, such as cluster expansion [9], particle-swarm optimization [44,45], and structure recognition algorithm [10] combined with first-principles calculations, have been performed to search the low-lying 2D flat boron structure, which reveal that there are only three phases ($\upsilon_{1/8}$, $\upsilon_{4/33}$, and $\upsilon_{2/15}$) more stable than the α monolayer [7] by several meV per B atom [41].

As shown in the middle of Fig. 2, the well-known α monolayer possesses similar symmetry (D_{6h}) to graphene, which can be viewed as a 2D form of the unfolded B_{80} fullerene [46], while the $\upsilon_{2/15}$ is constructed by the B nanoribbons with mirror symmetry [see Fig. 2(a)], and the width (WD) of the ribbons is defined by the number of hexagonal vacancy along the connecting line (light blue line). Insight into the $\upsilon_{2/15}$ monolayer, the ribbon-type building blocks are derived from α monolayer with appropriate tailoring (WD = 2). Furthermore, we have revealed that the $\upsilon_{1/8}$ monolayer [see Fig. 2(b)] is constructed by the α ribbon of WD = 3, and the $\upsilon_{4/33}$ monolayer (see Fig. S1) is assembled by the α ribbon of WD = 4. Thus, we can propose a modeling strategy to design stable boron monolayer candidates with LDs based on the self-assembly of α ribbons [see Fig. 2(c)]. We set the number of ribbon-type building blocks in the repeat unit as N ($N \geqslant 2$), and the width of any α ribbon is $n_i (n_i \geqslant 2)$. As the B atoms in the above configurations contain three types of coordination (CN = $4 \sim 6$), the new 2D phases belong to the β-type boron monolayers [44]. For the sake of distinction, any monolayer constructed by the self-assembly of N α ribbons is named $\beta_{n_1-n_2-\ldots-n_N} (n_i \geqslant 2; N \geqslant 2)$, and the three stable boron monolayers can be described as β_{2-2} ($\upsilon_{2/15}$), β_{3-3} ($\upsilon_{1/8}$), and β_{4-4} ($\upsilon_{4/33}$), respectively. Notably, the relationship between the hexagonal vacancy density and the number of α ribbons in the cell can be described as a general formula as shown in the inset of Fig. 2.

According to the modeling rule illustrated in Fig. 2(c), initial candidates of infinite 2D boron can be designed without constraints. Considering the convenience of subsequent research, we restrict N in a small range of $2 \leqslant N \leqslant 4$, and the total number of B atoms in the unit cell is smaller than 120. Combined with the above constraints, we have screened all the potential configurations in Table S1. The initial structures have been completely optimized for both the lattice constants and the atomic positions by the first-principle calculations.

As shown in Fig. 3(a), we have plotted the average formation energy (E_{form}) of the designed boron monolayers as a function of vacancy density (υ). Interestingly, all the phases constructed by the self-assembly of α ribbons are more stable than the highly symmetric α monolayer, which indicated the unusual LDs are intrinsic in these 2D boron family. The β_{2-2} ($\upsilon_{2/15}$) monolayer is the isomer with the highest density of LDs, and α monolayer is the other limit. Clearly, the most stable boron monolayers correspond to the optimal vacancy density (υ), which indicated that the proper distribution of LDs is critical for the stability of boron monolayers. Insight into Fig. 3 shows the lowest configurations with ($N = 2 \sim 4$) are β_{4-4}, β_{3-4-4} (see Fig. S1), and $\beta_{3-3-3-4}$, respectively. Furthermore, the proposed long-range order stable phase ($\beta_{3-3-3-4}$) owns superior thermal stability at high temperatures, which can be proved by the AIMD simulations in Fig. S2. In addition, based on the strategy of LDs engineering, we have searched new boron monolayers more stable than the always-believed ground-state β_{3-3} at the fixed $\upsilon_{1/8}$ [9,10], and the corresponding phases are highlighted in yellow in Table S1. Undoubtedly, compared with the three ground-state phases (β_{2-2}, β_{3-3}, and β_{4-4}) searched by

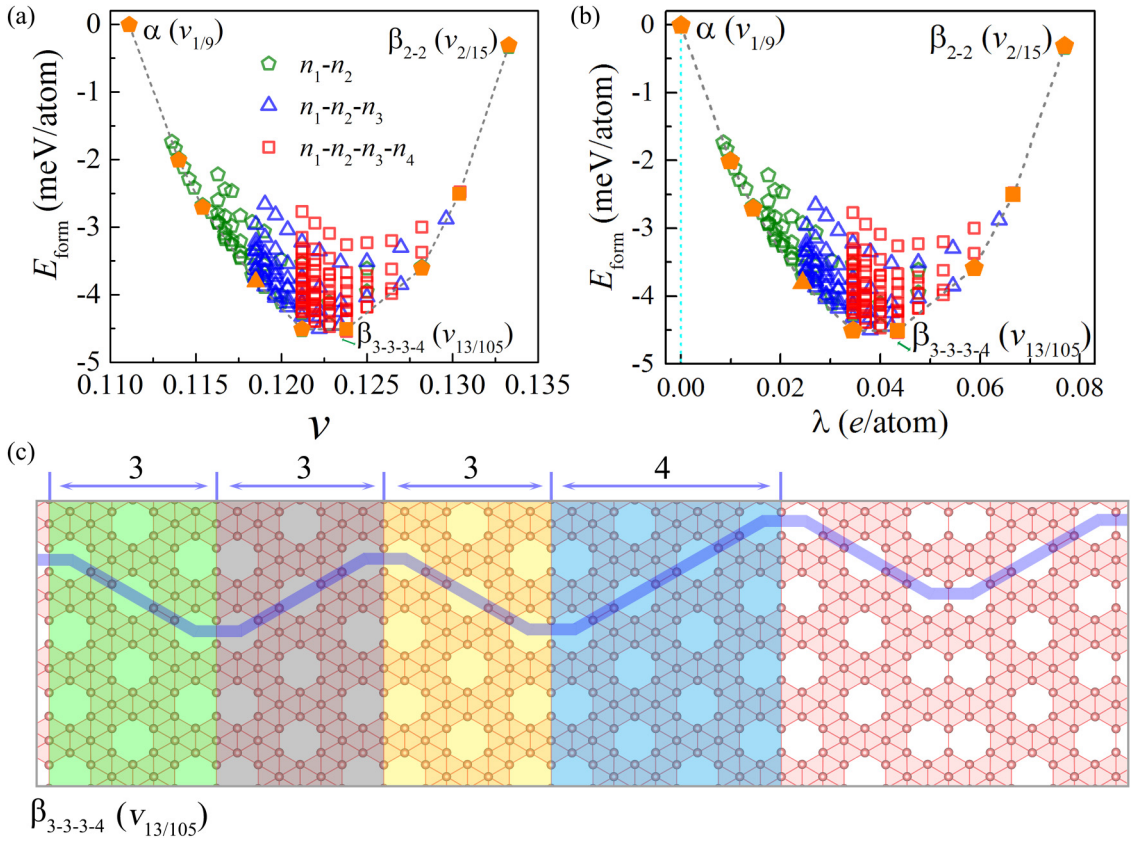

FIG. 3. (a) The average formation energies E_{form} of boron monolayers as a function of the vacancy density υ, and the three kinds of hollow dots represent three type combinations. (b) The average formation energies E_{form} as a function of the AEC parameter λ. The α monolayer is set as the reference phase in (a), (b), which is set to zero. (c) The formation mechanism of $\beta_{3-3-3-4}$ monolayer based on the α ribbons self-assembly.

various expensive searching algorithms, we have proposed a simple universal rule to design stable boron monolayers based on the self-assembly of α ribbons. Within this framework, countless boron monolayers based on LDs engineering more stable than α monolayer can be formed, which declares the polymorphism of boron monolayers. To describe the local atomic environments of boron monolayers, we have developed an average electron compensation (AEC) mechanism to prescreen the reasonable candidates [10], where the optimal value of AEC descriptor (λ) for stable boron monolayers is close to zero in general. However, the relationship of E_{form} and λ in Fig. 3(b) indicated that the reasonable AEC parameters for these stable 2D boron isomers are located in a very small electron-deficient range, and the similar parabolas in Figs. 3(a) and 3(b) may be due to the similarity of the local motifs in these designed boron monolayers.

Compared to other 2D materials, the inclusion of LDs is a positive factor in boron monolayers. As the left neighbor of carbon in the periodic table, boron cannot form stable honeycomb nanostructures like carbon due to electron deficiency. The proposed stable B_{80} cage is based on doping additional B atom in the center of each hexagon in B_{60} fullerene, and the famous α monolayer derived from doping B atom in the honeycomb lattices. It is widely believed that an ideal boron monolayer should be isoelectronic to graphene, which indicated the optimal charge distribution [47]. Based on the simple electron counting rule and vacancy density relationship, Zhang *et al.* have deduced that the ground-state vacancy density is $\upsilon_{1/9}$ [48]. Similarly, the AEC analysis demonstrated that the α monolayer is the best isomer with $\lambda = 0$ [10], while the calculation results in Fig. 3 declared that the former theory and mechanism for boron monolayers might be deficient, which only accounts for the general case at a relatively big range of υ.

To gain a detailed insight into the LDs-dependent stability of the above 2D boron, we have calculated the projected density of states (PDOS) for the five representative boron monolayers [see Fig. 4(a)]. As we know, the former analysis of Fermi level (E_F) lying in the gap of in-plane ($s + p_{x,y}$) bonding states cannot be used to understand the stability of boron monolayers, which is because these features widely exist in various proposed boron monolayers [10]. A recent theory proposed that the hybridization among out-of-plane boron p_z orbitals is crucial for determining the relative stability of the boron monolayers at a small range [48]. As shown in Fig. 4(a), compared with the in-plane orbitals, the out-of-plane p_z states cross the E_F, which indicates the metallic property of the above boron monolayers is rooted in the delocalized π states. According to the definition of bondinglike and antibondinglike states for p_z orbitals, the hybrid p_z states in boron monolayers can be marked as π and π^* [48], and the hybridization of p_z orbitals results in a dip near the E_F, which is confined to the peaks of π and π^* states. According to the analysis for p_z states, the less stable α monolayer is due to

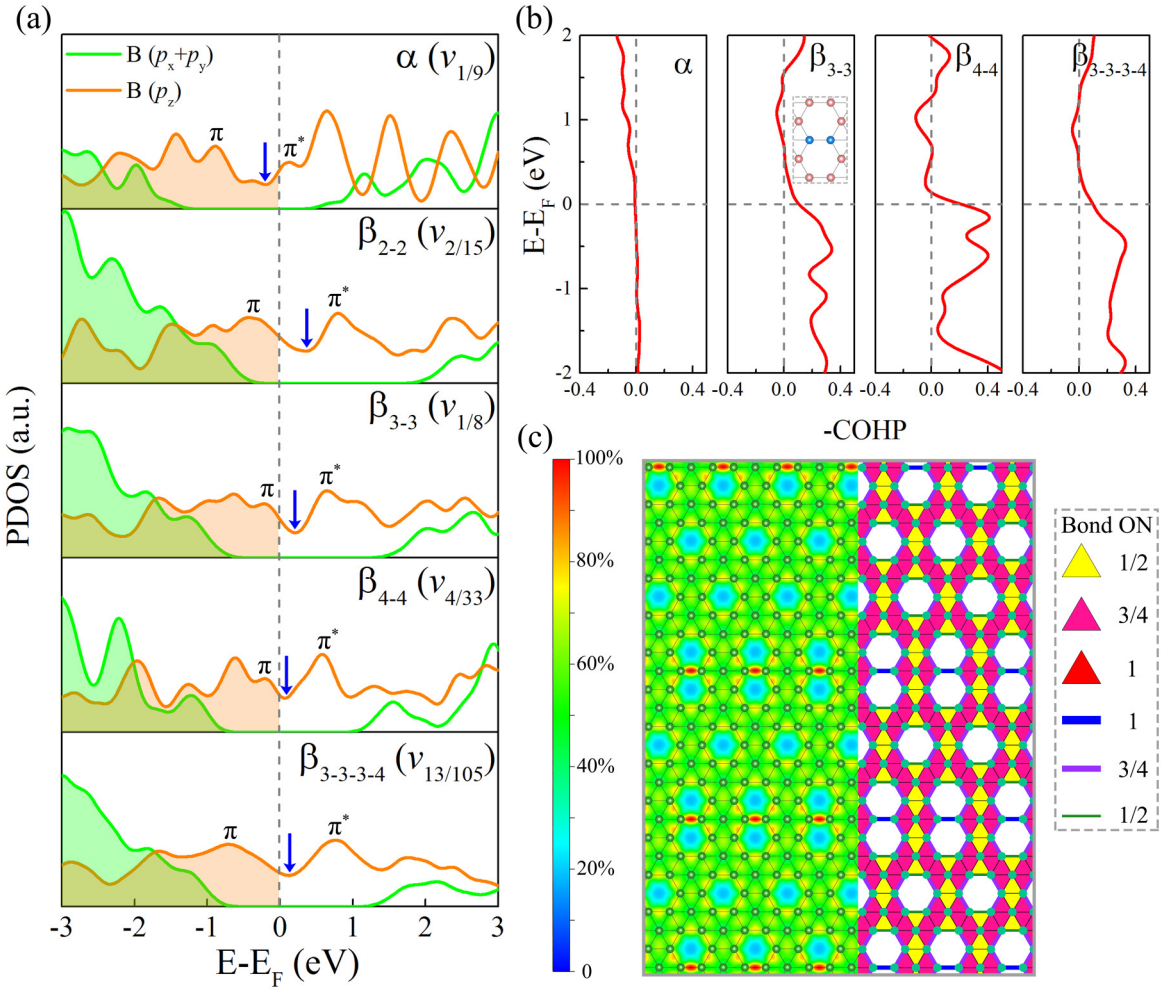

FIG. 4. (a) PDOS of the five boron monolayers. The green lines show the $(p_x + p_y)$ states, and the orange lines represent the out-of-plane p_z states. Arrows mark the dip in the p_z states near the E_F. (b) The COHP plots for the four boron monolayers. (c) Bonding analysis for the $\beta_{3-3-3-4}$ monolayer. The left part shows the charge difference, and the right part shows the possible 2c–2e and 3c–2e bond distributions. The percentages of the color bar are signed with the peak amplitude value for the isosurface located at the left side, and the occupation numbers (ON) of the 2c–2e and 3c–2e bonds are listed on the right side.

the partially occupied antibonding π^* states (electron excessive) and the unfavorable β_{2-2} ($\upsilon_{2/15}$) monolayer is electron deficient as the E_F cut the bonding π states. Based on the proposed descriptor $|E_{dip} - E_F|$, the optimal boron monolayers correspond to the lowest $|E_{dip} - E_F|$ value [48]. The stability of β_{3-3}, β_{4-4}, and $\beta_{3-3-3-4}$ can be qualitatively understood by this hybridization mechanism of p_z states, due to the relatively small value of $|E_{dip} - E_F|$ [see Fig. 4(a)]. Thus, the stability of boron monolayers cannot be understood by a simple model or any single variable, according to the above PDOS analysis.

Since the LDs can enhance the stability of these phases, here we plot crystal orbital Hamilton populations (COHP) [49,50], based on the first-principles calculations to show the significance of the bonding interaction at the LDs. For comparison, we plot the COHP of B–B bond formed by the hexagonal B atom (CN = 5) and the inner B atom (CN = 6) for α monolayer, and the COHP of the B–B bond shared by two hexagon vacancies (CN = 4) at the LDs for the three stable phases [see Fig. 4(b)]. Clearly, the bonding interaction in α monolayer is negligible, while the counterparts in the three β-type boron monolayers are much stronger, which can be identified by the obvious bonding peaks. In addition, the contributed value of the B–B bond at the LDs to the stability of the boron monolayer can be reflected by the electron localization. In Fig. 4(c), we show the charge difference of the $\beta_{3-3-3-4}$ monolayer, the region of electron localization is represented by the warm color. Combined with the AEC model analysis, we find a set of possible discrete occupation number for the two-center two-electron (2c–2e) and three-center two-electron (3c–2e) bond to fulfill the octet rule for $\beta_{3-3-3-4}$ monolayer. In particular, the model solution presents the electron localization of the LDs with a maximum occupation number of 1 for the 2c–2e bond, which indicated the significance of the bonds formed by two adjacent hexagonal vacancies at the LDs regions.

Under suitable growth conditions, 2D boron phases formed by the self-assembly of the LDs in β_{12} ($\upsilon_{1/6}$) and χ_3 ($\upsilon_{1/5}$) monolayers have been observed in the recent experiments on Ag (111) substrates [19]. Hence, a systematic study of the structural stability of the new boron monolayers based on LDs engineering from β_{12} (A) and χ_3 (B) monolayers is of urgent need. Here we focused on the simplest model

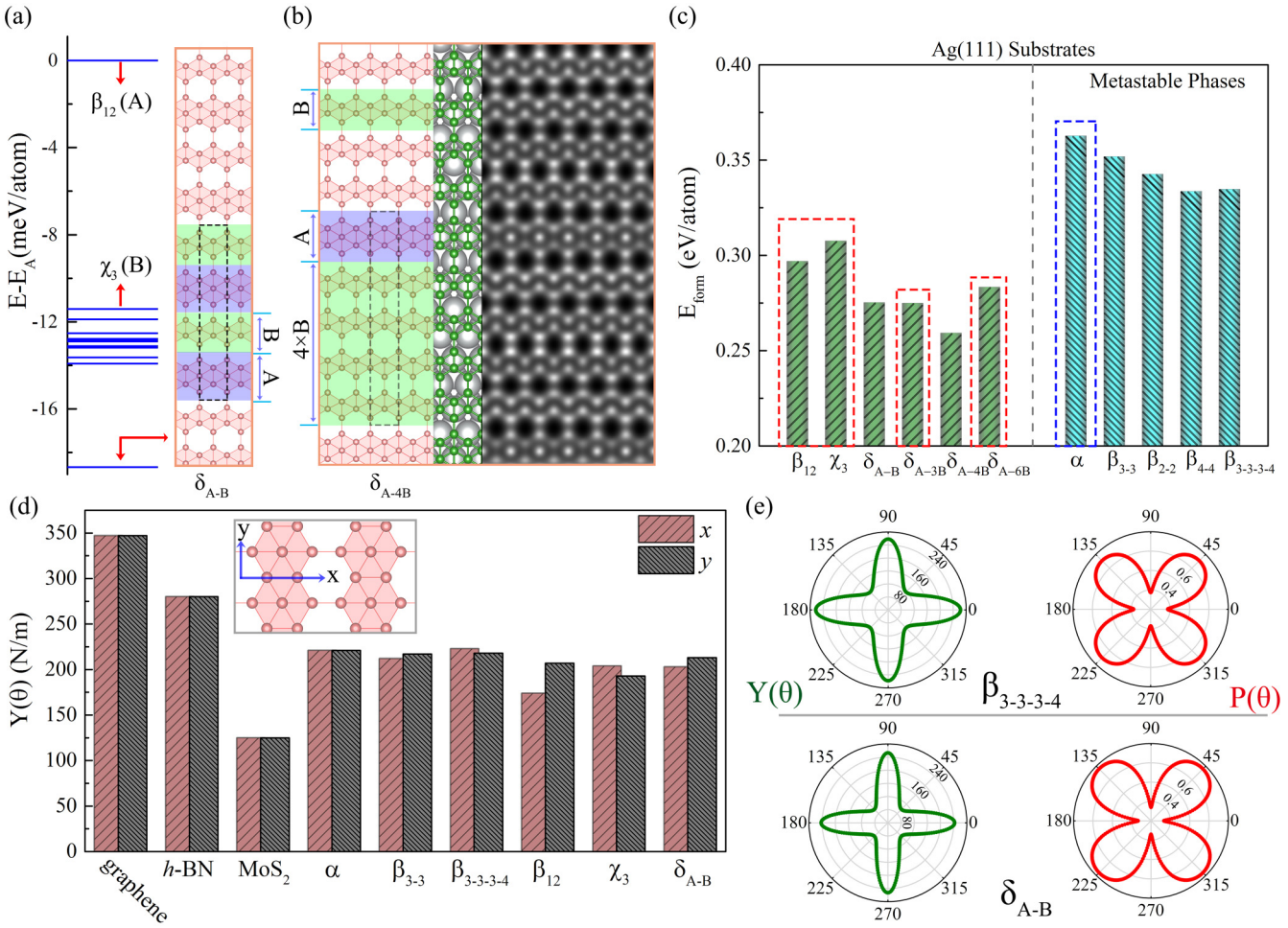

FIG. 5. (a) Configurational energy spectra of the δ_{A-n*B} boron monolayers, and the formation mechanism of δ_{A-B} monolayer. (b) The formation mechanism of δ_{A-4B} monolayer; the right part represents the top view of the δ_{A-4B} monolayer on the Ag (111) substrates and the corresponding simulated STM image. (c) The average formation energy of the boron monolayers on the Ag (111) substrates; the bars highlighted with dashed lines represent the current experimental phases. (d) Calculated Young's modulus for the typical 2D materials and several boron monolayers; x and y correspond to the armchair and zigzag directions for the honeycomb lattice. (e) Calculated orientation-dependent Young's modulus Y(θ) in N/m and Poisson's ratio P(θ) for the two boron monolayers.

of binary ribbons assembled ($\delta_{m*A-n*B}$) in the unit cell with ($1 \leqslant m,\ n \leqslant 10$), and the details of all the designed phases are presented in Table S2. Although all the optimized phases are more stable than β_{12}, the majority of boron monolayers in Table S2 are less stable than χ_3 monolayer (see Fig. S3), while the special family of δ_{A-n*B} boron monolayers [see Fig. 5(a)] are more stable than both their parent structures, and the δ_{A-B} boron monolayer is more stable than other phases by 5 meV per atom. Clearly, the above calculated results indicated the LDs energetically favor spatially periodic self-assembly, which highlights the important role of LDs in boron monolayers.

To explore the possibility of new boron monolayers fabricated in the experiments, we have studied the structural stability of several representative boron monolayers deposited on the Ag substrates (the optimized structures are shown in Fig. S4 and S5). As shown in Fig. 5(c), the calculated average formation energy (E_{form}) of the designed boron monolayers with LDs (left side) on the Ag (111) substrates are more stable than the experimental β_{12} and χ_3 monolayers, and the counterpart of monolayers assembled by the α ribbons (right side) are more stable than the metastable α monolayer [18]. It is worth to note that the E_{form} of δ_{A-4B} boron monolayer is about 48 meV/atom lower than the experimental χ_3 monolayers, and two predicted combination products (δ_{A-3B} and δ_{A-6B}) have been observed on the Ag (111) substrates recently [19]. Since the lower E_{form} of δ_{A-4B} indicated its potential for experimental synthesis, we have simulated the scanning tunnel microscopy (STM) image [see Fig. 5(b)] for the δ_{A-4B}/Ag(111) system, which may provide some references for future experiments. Thus, the results of the E_{form} demonstrated that the 2D boron phases with LDs could be fabricated under proper conditions, which are due to their better performance on Ag substrates than the current experimental ground-state and metastable phases. Combined with the results of free-standing boron monolayers in Fig. 3 and the stability of boron monolayers on Ag (111) substrates, we are inclined to believe that the stable boron monolayers (with/without substrates) should be long-range disorder, which do not exist in a smallest unit like graphene/h-BN. It

should be noted that, in theory, various boron monolayers can be fabricated by controlling the growth substrates and the experimental conditions, elaborately [39,41]. Hence, our results demonstrate that there are a number of opportunities to realize synthetic polymorphic boron monolayers in the future.

Considering the practical application, 2D materials should exhibit high levels of flexibility against off-plane deformation, and we have performed first-principles analysis of the mechanical properties for these boron monolayers. Although the engineering strain can be applied in any lattice orientation, here we focused on the common case with applying strains along the x and y directions. As we know, the orientation-dependent elastic response depends on structural symmetry; thus, these typical 2D materials (graphene, h-BN, and MoS_2) with high symmetry share the identical Young modulus [$Y(\theta)$] along x/y directions [see Fig. 5(d)]. However, the $Y(\theta)$ of boron monolayers are lower than graphene and h-BN, which are higher than the ones in MoS_2. The former simulations revealed a ∼50% strength reduction due to the presence of the LDs between the polygonal graphene domains [37], which indicated the negative effect of the LDs. However, the boron monolayers with LDs formed by the ribbon self-assembly have better mechanical properties. As shown in Fig. 5(d), the $Y(\theta)$ along the x direction of the $\beta_{3-3-3-4}$ monolayer is higher than the ones in the α monolayer, and the counterpart in δ_{A-B} along the y direction also exhibits superiority over the pristine β_{12} and χ_3 monolayers. To gain a comprehensive description of the anisotropic mechanical properties for the boron monolayers, the orientation-dependent Young's modulus and Poisson ratio were calculated and presented in 2D polar representation curves. Figure 5(e) shows that both the boron monolayers share similar maximal/minimal $Y(\theta)$, and the insensitive $Y(\theta)$ to υ [in Fig. 5(d)] is due to the similar coordination environments and B–B bond length in the above boron monolayers, which agrees with the former theoretical investigation [51]. Notably, the β_{12} monolayer has been reported to possess a high specific modulus close to graphene [51], and the β_{12} monolayer also can be formed by the self-assembly of α ribbons with (WD = 1) [see Fig. S1(a)]. Our findings uncover the special value of LDs to modulate the mechanical response of boron monolayers than other conventional 2D materials, which indicates the potential application of boron monolayers for advanced flexible electronic devices.

Combining the above information of structures and properties, we have abstracted a simple rule to optimize stability, mechanical properties, and electronic properties via quantitative line defects engineering with the self-assembly of α ribbons ($n_i = 3, 4$), and the monolayer in this family can be defined as $\beta_{n_1-n_2-\ldots-n_N}$ ($n_i = 3, 4; N \geqslant 2$). Thus, we have calculated the constructed monolayers with ($2 \leqslant N \leqslant 7$), and all the 2D phases exhibit excellent stability with $E_{form} < -5.998\,eV/atom$, as listed in Table S3. Accordingly, due to the similar vacancy concentration and local motifs, all the boron monolayers in this family may demonstrate comparable mechanical properties and electronic properties.

IV. CONCLUSIONS

In summary, we have demonstrated the unusual positive role of LDs in boron monolayers based on the first-principles calculations, in contrast to the conventional 2D materials. Based on the self-assembly of α ribbons, we have developed a simple universal rule to construct infinite stable free-standing boron monolayers, and a long-range order stable phase $\beta_{3-3-3-4}$ monolayer is obtained. Combined with the COHP analysis, we have detected the special value of the LDs to the stability of the boron monolayers. In addition, we have systematically investigated the possible binary combination structures constructed by the LDs engineering from β_{12} and χ_3 monolayers, and several highly stable boron monolayers on the Ag (111) substrates have been uncovered. Furthermore, in contrast to other 2D materials, LDs in boron monolayers may make a positive contribution to enhance the mechanical properties of the systems. Moreover, we have abstracted a simple rule to optimize stability, mechanical properties, and electronic properties based on the self-assembly of α ribbons ($n_i = 3, 4$). Our findings provide a valuable angle to understand the special role of LDs in boron monolayers, which may stimulate the further development of 2D boron research, and the determinant in long-range disorder boron monolayers deserves deeper exploration. Remarkably, the designed stable boron monolayers with a higher mechanical response may be used to design flexible electronic devices in the future.

ACKNOWLEDGMENTS

This work was supported by the National Natural Science Foundation of China (Grant No. 11974160), the Guangdong Natural Science Funds for Distinguished Young Scholars (Grant No. 2017B030306008), the Guangdong Provincial Key Laboratory of Computational Science and Material Design (Grant No. 2019B030301001), the Guangdong-Hong Kong-Macao Joint Laboratory (Grant No. 2019B121205001), and Key-Area Research and Development Program of Guangdong Province (Grant No. 2020B010183001). The computer time at the Center for Computational Science and Engineering of Southern University of Science and Technology is gratefully acknowledged.

[1] O. V. Yazyev and Y. P. Chen, Nat. Nanotechnol. **9**, 755 (2014).
[2] X. Zou and B. I. Yakobson, Acc. Chem. Res. **48**, 73 (2014).
[3] W. Yao, B. Wu, and Y. Liu, ACS Nano **14**, 9320 (2020).
[4] L. Kou, C. Tang, W. Guo, and C. Chen, ACS Nano **5**, 1012 (2011).
[5] X. Li, X. Wu, X. C. Zeng, and J. Yang, ACS Nano **6**, 4104 (2012).
[6] Y. Liu, X. Zou, and B. I. Yakobson, ACS Nano **6**, 7053 (2012).
[7] H. Tang and S. Ismail-Beigi, Phys. Rev. Lett. **99**, 115501 (2007).
[8] X. Yang, Y. Ding, and J. Ni, Phys. Rev. B **77**, 041402(R) (2008).
[9] E. S. Penev, S. Bhowmick, A. Sadrzadeh, and B. I. Yakobson, Nano Lett. **12**, 2441 (2012).

[10] S.-G. Xu, X.-T. Li, Y.-J. Zhao, J.-H. Liao, H. Xu, and X.-B. Yang, Nanoscale **10**, 13410 (2018).

[11] Y. Wang, Y. Park, L. Qiu, I. Mitchell, and F. Ding, J. Phys. Chem. Lett. **11**, 6235 (2020).

[12] Y. Liu, E. S. Penev, and B. I. Yakobson, Angew. Chem. Int. Ed. Engl. **52**, 3156 (2013).

[13] Z. Zhang, Y. Yang, G. Gao, and B. I. Yakobson, Angew. Chem. Int. Ed. Engl. **54**, 13022 (2015).

[14] A. J. Mannix, X.-F. Zhou, B. Kiraly, J. D. Wood, D. Alducin, B. D. Myers, X. Liu, B. L. Fisher, U. Santiago, J. R. Guest, M. J. Yacaman, A. Ponce, A. R. Oganov, M. C. Hersam, and N. P. Guisinger, Science **350**, 1513 (2015).

[15] B. J. Feng, J. Zhang, Q. Zhong, W. B. Li, S. Li, H. Li, P. Cheng, S. Meng, L. Chen, and K. H. Wu, Nat. Chem. **8**, 563 (2016).

[16] S. G. Xu, Y. J. Zhao, J. H. Liao, X. B. Yang, and H. Xu, Nano Res. **9**, 2616 (2016).

[17] Z. Zhang, A. J. Mannix, X. Liu, Z. Hu, N. P. Guisinger, M. C. Hersam, and B. I. Yakobson, Sci. Adv. **5**, eaax0246 (2019).

[18] Z. Qing, Z. Jin, C. Peng, F. Baojie, L. Wenbin, S. Shaoxiang, L. Hui, M. Sheng, C. Lan, and W. Kehui, J. Phys.: Condens. Matter **29**, 095002 (2017).

[19] X. Liu, Z. Zhang, L. Wang, B. I. Yakobson, and M. C. Hersam, Nat. Mater. **17**, 783 (2018).

[20] X. Liu, L. Wang, S. Li, M. S. Rahn, B. I. Yakobson, and M. C. Hersam, Nat. Commun. **10**, 1642 (2019).

[21] L. Liu, Z. Zhang, X. Liu, X. Xuan, B. I. Yakobson, M. C. Hersam, and W. Guo, Nano Lett. **20**, 1315 (2020).

[22] A. P. Sergeeva, I. A. Popov, Z. A. Piazza, W. L. Li, C. Romanescu, L. S. Wang, and A. I. Boldyrev, Acc. Chem. Res. **47**, 1349 (2014).

[23] W.-L. Li, X. Chen, T. Jian, T.-T. Chen, J. Li, and L.-S. Wang, Nat. Rev. Chem. **1**, 0071 (2017).

[24] G. Kresse and J. Furthmüller, Phys. Rev. B **54**, 11169 (1996).

[25] G. Kresse and D. Joubert, Phys. Rev. B **59**, 1758 (1999).

[26] J. P. Perdew, K. Burke, and M. Ernzerhof, Phys. Rev. Lett. **77**, 3865 (1996).

[27] S. Nosé, J. Chem. Phys. **81**, 511 (1984).

[28] See Supplemental Material at http://link.aps.org/supplemental/10.1103/PhysRevMaterials.5.044003 for the details of the constructed boron monolayers, the AIMD simulations of $\beta_{3-3-3-4}$ monolayer, and optimized atomic structures of the B/Ag(111) systems.

[29] K. S. Novoselov, D. Jiang, F. Schedin, T. J. Booth, V. V. Khotkevich, S. V. Morozov, and A. K. Geim, Proc. Natl. Acad. Sci. USA **102**, 10451 (2005).

[30] A. H. C. Neto and K. Novoselov, Rep. Prog. Phys. **74**, 082501 (2011).

[31] N. D. Mermin, Phys. Rev. **176**, 250 (1968).

[32] J. Lahiri, Y. Lin, P. Bozkurt, I. I. Oleynik, and M. Batzill, Nat. Nanotechnol. **5**, 326 (2010).

[33] X. Ren, X. Wang, and C. Jin, Nano Lett. **19**, 8581 (2019).

[34] A. M. van der Zande, P. Y. Huang, D. A. Chenet, T. C. Berkelbach, Y. You, G.-H. Lee, T. F. Heinz, D. R. Reichman, D. A. Muller, and J. C. Hone, Nat. Mater. **12**, 554 (2013).

[35] S. Wang, G.-D. Lee, S. Lee, E. Yoon, and J. H. Warner, ACS Nano **10**, 5419 (2016).

[36] Y. Wei, J. Wu, H. Yin, X. Shi, R. Yang, and M. Dresselhaus, Nat. Mater. **11**, 759 (2012).

[37] Z. Song, V. I. Artyukhov, B. I. Yakobson, and Z. Xu, Nano Lett. **13**, 1829 (2013).

[38] Z. Song, V. I. Artyukhov, J. Wu, B. I. Yakobson, and Z. Xu, ACS Nano **9**, 401 (2014).

[39] Z. Zhang, E. S. Penev, and B. I. Yakobson, Chem. Soc. Rev. **46**, 6746 (2017).

[40] S.-G. Xu, X.-T. Li, Y.-J. Zhao, J.-H. Liao, W.-P. Xu, X.-B. Yang, and H. Xu, J. Am. Chem. Soc. **139**, 17233 (2017).

[41] A. J. Mannix, Z. Zhang, N. P. Guisinger, B. I. Yakobson, and M. C. Hersam, Nat. Nanotechnol. **13**, 444 (2018).

[42] R. Wu, I. K. Drozdov, S. Eltinge, P. Zahl, S. Ismail-Beigi, I. Bozovic, and A. Gozar, Nat. Nanotechnol. **14**, 44 (2019).

[43] W. Li, L. Kong, C. Chen, J. Gou, S. Sheng, W. Zhang, H. Li, L. Chen, P. Cheng, and K. Wu, Sci. Bull. **63**, 282 (2018).

[44] X. Wu, J. Dai, Y. Zhao, Z. Zhuo, J. Yang, and X. C. Zeng, ACS Nano **6**, 7443 (2012).

[45] X. Yu, L. Li, X.-W. Xu, and C.-C. Tang, J. Phys. Chem. C **116**, 20075 (2012).

[46] N. Gonzalez Szwacki, A. Sadrzadeh, and B. I. Yakobson, Phys. Rev. Lett. **98**, 166804 (2007).

[47] Y. Jiao, F. Ma, J. Bell, A. Bilic, and A. Du, Angew. Chem. Int. Ed. **55**, 10292 (2016).

[48] Z. Zhang, S. N. Shirodkar, Y. Yang, and B. I. Yakobson, Angew. Chem. Int. Ed. **56**, 15421 (2017).

[49] V. L. Deringer, A. L. Tchougreeff, and R. Dronskowski, J. Phys. Chem. A **115**, 5461 (2011).

[50] S. Maintz, V. L. Deringer, A. L. Tchougreeff, and R. Dronskowski, J. Comput. Chem. **37**, 1030 (2016).

[51] Z. Zhang, Y. Yang, E. S. Penev, and B. I. Yakobson, Adv. Funct. Mater. **27**, 1605059 (2017).